Nanoscale

PAPER

View Article Online
View Journal | View Issue

Cite this: *Nanoscale*, 2025, **17**, 20157

Engineering mechanical strength and resistance to fatigue of a nanostructured protein material through genetic removal of electrostatic repulsions

Judith Escrig, Juan Carlos Gil-Redondo, Alejandro Valbuena* and Mauricio G. Mateu *

Protein nanoarrays and other protein-based nanostructures are being developed for many biomedical and technological applications. However, many protein assemblies are prone to disruption under load, and susceptible to material fatigue. Acquisition of a fundamental knowledge on the relationship between structure and mechanical properties of protein assemblies may guide the engineering of protein nanostructures with a higher strength and resistance to fatigue. The capsid protein (CA) of the human immunodeficiency virus can self-assemble into a single molecule-thick, flexible nanoarray that can coat large surfaces. In this study, a genetic engineering strategy was used to individually remove in the CA protein array the side chain of 7 amino acid residues per subunit involved in intermolecular interactions. The effects of eliminating those side chains, and their intermolecular interactions, on the equilibrium dynamics, stiffness, strength, and resistance to fatigue of the CA nanoarray were quantified using atomic force microscopy. The results revealed that removal of different types of attractive intermolecular interactions (van der Waals contacts, hydrogen bonds, and/or ionic bonds), increased the conformational flexibility of the protein array, and decreased its stiffness and strength. In contrast, removal of a naturally occurring, repulsive charge–charge intermolecular interaction in the nanoarray actually led to dramatic increases in strength against point loads (by ~60%) and resistance to fatigue (by ~50%), without increasing its stiffness. These findings suggest a general genetic strategy to increase the intrinsic strength and resistance to fatigue of nanostructured protein materials, based on the optimization of the ionic interactions between subunits.

Received 11th June 2025,
Accepted 14th August 2025

DOI: 10.1039/d5nr02490k

rsc.li/nanoscale

Introduction

Protein-based nanomaterials are being explored for a plethora of applications in biomedicine, biotechnology, and nanotechnology.[1–6] These biomaterials include one-dimensional (1D), two-dimensional (2D), and three-dimensional (3D) nanostructured arrays of bound protein molecules, either found in nature or designed in the laboratory.

Protein-based nanostructures are endowed with a number of features that make them potentially advantageous relative to other materials for many biomedical or industrial applications.[7] Their strengths include: (i) spontaneous and efficient self-assembly and disassembly under controlled conditions; (ii) monodispersity and well-defined composition and architecture; (iii) inbuilt chemical and biological functionalities (*e.g.*, a high affinity and specificity for a particular ligand molecule, or programmed entry into a particular cell or cell compartment); (iv) propensity to undergo controlled conformational rearrangements; (v) adequacy for engineering structural or functional modifications to suit a particular application, using chemical approaches and/or genetic strategies (site-directed mutagenesis or directed evolution); (vi) reproducible and economical large-scale production; (vii) biocompatibility, absence of toxicity, and biodegradability.

However, protein-based materials may also present some serious weaknesses for many intended applications. In particular, many protein assemblies are "soft" materials,[8] held together by weak intermolecular non-covalent interactions and, thus, prone to disruption by point loads or mechanically induced material fatigue.[9] Material fatigue is the most common cause of failure of many materials,[10] and different protein assemblies appear indeed to be highly sensitive to fatigue, elicited even by weak forces.[9,11–13] From a practical

Centro de Biología Molecular "Severo Ochoa" (CSIC-UAM), Universidad Autónoma de Madrid, 28049 Madrid, Spain. E-mail: mauricio.garcia@uam.es, mgarcia@cbm.csic.es, avalbuena@cbm.csic.es

standpoint, resistance to compression and tension stress and material fatigue should be taken into account, for example, when designing protein-based biocompatible coatings of implants for cell tissue regeneration, as the implant will be repeatedly bent and stretched.[14] Some natural protein assemblies do show a very high mechanical strength. They include fibrous (1D) proteins such as fibroin, keratin, or collagen, but also 3D complexes such as some bacteriophage capsids.[9] These and other naturally evolved protein assemblies provided the first indication that protein complexes can be made stronger through genetic mutation. While some natural proteins may be mechanically strong enough, they may not possess the adequate architecture or functionality required for the intended applications in biomedicine or the industry. These and other considerations encourage the acquisition of the fundamental knowledge needed to guide the engineering of natural and artificial protein-based nanostructures with high enough mechanical strength and resistance to fatigue.[15,16]

Protein-based 2D nanostructures in particular are being developed for many uses, including functionalized, biocompatible coatings of inert materials for cell tissue regeneration, antifouling coatings, molecular nanosieves with pores of a precisely defined size, and biosensors.[17–21] Natural protein-based 2D nanostructures include S-layers, which are biologically relevant envelopes of certain microorganisms.[22] An example of artificial protein-based 2D nanostructures is provided by computationally designed nanosheets self-assembled from engineered protein STM4215 hexamers from *S. typhimurium*.[23] The capsid protein (CA) of human immunodeficiency virus type 1 (HIV-1) can readily and efficiently self-assemble onto an inorganic substrate as a single-molecule thick, 2D nanostructure that can coat very large surfaces[24] (Fig. 1). This extended nanocoating is arranged as a regular, hexameric protein lattice that reproduces the fundamental CA lattice of the authentic HIV-1 capsid,[25] but without the pentameric "defects" that allow, in the maturing virion, the closure of the lattice into a cone-shaped nanoparticle. The CA-based protein monolayer constitutes an interesting addition to the still limited, but rapidly growing number of available 2D protein nanostructures.

There are few studies on the molecular determinants of the mechanical properties of protein nanostructures in general,[9] and of 2D protein nanoarrays in particular. Regarding HIV-1, Dr Itay Rousso and colleagues found that immature virions are stiffer than mature virions, revealing that softening of the virion is required for infection.[26] The differences in stiffness were due to the effect of the C-terminal domain of the Env protein, which is embedded in the viral lipid envelope and does not form a part of the virus capsid. No comparison of mechanical properties between the immature, spherical retroviral capsid made of the Gag polyprotein and the cone-shaped mature capsid made of CA is available. While both Gag-based and CA-based 2D nanoarrays could provide interesting protein-based materials, conditions for assembly have been found for the CA-based array only. Our previous mechanical analyses have shown that the natural CA protein 2D lattice is highly sensitive to mechanical disruption and material fatigue,[13,24] as also observed for other protein-based assemblies.[9,11,12] The CA protein lattice provides, thus, an excellent model system to investigate, at the atomic level, the structural determinants of the mechanical properties of protein-based nanostructures and, more specifically, 2D protein arrays. It also provides a model to investigate different strategies to engineer the mechanical properties of a protein assembly. The knowledge acquired may help guiding the development by rational engineering of modified protein-based materials with increased mechanical strength and resistance to fatigue.

The HIV-1 CA protein monomer consists of a N-terminal domain (NTD) and a C-terminal domain (CTD) connected by a flexible peptide segment (Fig. 1A). In the hexagonal CA lattice, CA monomers are organized as hexamers in which the mono-

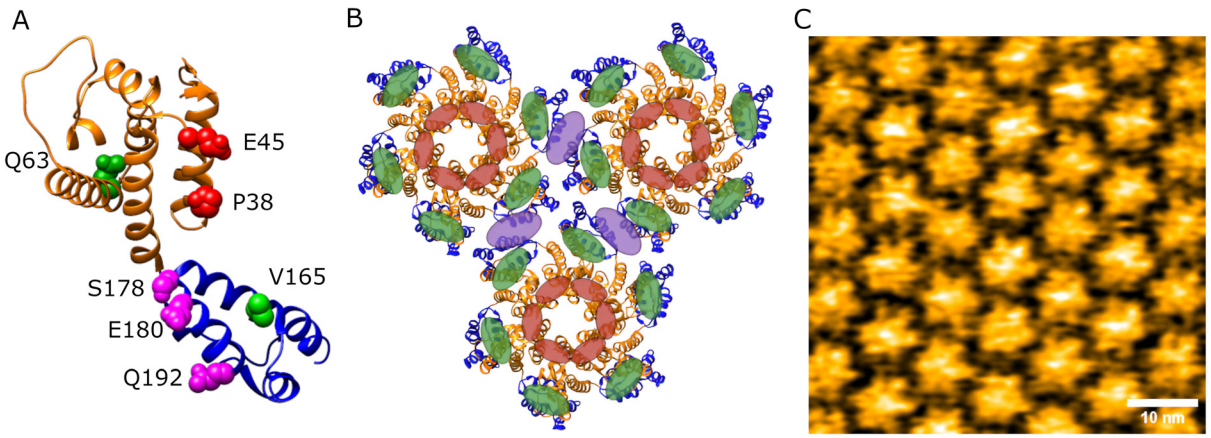

Fig. 1 The nanostructured CA protein lattice. (A) Ribbon model of the CA protein monomer (PDB ID: 4XFX). The NTD and the CTD are respectively colored orange and blue. The 7 amino acid residues chosen for mutational analysis are depicted as space-filling models, labelled, and color coded (red, green, and purple, residues that respectively participate in NTD-NTD, NTD-CTD and CTD-CTD interfaces) (B) atomic structure of the CA protein lattice (PDB ID: 4XFX). Ovals identify NTD-NTD (red), NTD-CTD (green), and CTD-CTD (purple) interfaces. (C) High-resolution AFM image of the CA protein lattice. The scale bar is 10 nm long.

mers are bound through NTD-NTD and NTD-CTD interfaces, with each hexamer bound to the 6 neighbor hexamers through CTD-CTD interfaces (Fig. 1B).[25] The CA monolayer (Fig. 1C) interacts with a negatively charged (mica) substrate through charge–charge interactions, and its structural elements are relatively free to deform and undergo lateral movements on the solid substrate.[13,24]

The starting hypothesis for the present study was that the mechanical stiffness, strength and resistance to fatigue of a 2D nanostructured material made of identical protein subunits may largely depend on the number and types of intermolecular interactions established between its subunits. We have individually removed by genetic means, following a protein engineering approach, the side chain (beyond the Cβ) of 7 amino acid residues of each CA monomer that are involved in different intermolecular interactions in the HIV-1 CA protein lattice. The effects of removing those side chains, and the inter-protein interactions they establish in the CA lattice, on the equilibrium dynamics, stiffness, strength, and resistance to material fatigue of this 2D nanostructure were quantified using atomic force microscopy (AFM).

Experimental section

Introduction of amino acid substitutions in CA by site-directed mutagenesis

To introduce specific amino acid substitutions in CA, site-directed mutagenesis using the QuikChange II Site-Directed Mutagenesis kit (Stratagene) was performed on plasmid pWISBH10 containing the coding region of the HIV-1 (strain BH10) CA protein.[27] The presence of the desired mutations and the absence of other mutations was confirmed by DNA sequencing.

CA protein expression and purification

CA^{wt} and CA mutants were expressed in *E. coli* BL21(DE3) transformed with recombinant plasmids that contained the corresponding CA-coding sequence. Cells were grown at 37 °C, and protein expression was induced by incubation in the presence of 1 mM IPTG for 3 h at 37 °C. The cells were then harvested and kept at −20 °C until use. For the purification of CA^{wt} and CA mutants a previously described procedure was used.[27] Briefly, the cells were thawed, resuspended in 50 mM Tris-HCl pH = 8 containing 5 mM β-mercaptoethanol, and lysed by sonication. The cell debris were removed by centrifugation, and CA present in the soluble fraction was purified in three steps that respectively involved ammonium sulfate precipitation, ion exchange chromatography (SP-Sepharose, Amersham Biotech) and size exclusion chromatography (Superdex 75, Amersham Biotech). The purified protein solutions were dialyzed against PBS pH = 7.4, and kept at −80 °C until use. The purity of the CA proteins was estimated by SDS-polyacrylamide gel electrophoresis, and their concentration was determined by UV spectrophotometry.

Assembly of nanostructured CA monolayers for AFM analysis

Self-assembly of CA^{wt} and CA mutants into a flat nanostructured monolayer was performed essentially as previously described.[24] Briefly, a 60 μl droplet of a 0.7 μM purified CA solution in PBS pH = 7.4 was deposited on a freshly cleaved, negatively charged mica surface and incubated at room temperature for 90 min.

AFM-based imaging of CA monolayers

An atomic force microscope (Nanotec Electronica S.L.), controlled with WSxM[28] software and operated in Jumping Mode[29] was used for imaging of CA^{wt} and mutant CA assemblies in a liquid environment. Soft cantilevers with a nominal spring constant of 0.1 N m^{-1} (qpBioAC, Nanosensors), suitable for scanning biological samples, were used. The applied force during imaging was kept under ~40 pN.

AFM-based analysis of the equilibrium dynamics of CA monolayers

AFM images of the CA monolayers covering a surface of 150 × 150 nm were taken in Jumping Mode as previously described,[24] using a maximum force of 40 pN, and the distances between the centers of many neighbor hexamers in the monolayer were measured. This data set was then used to determine (i) the average distance between hexamer centers at equilibrium (the lattice parameter a_i); and (ii) the width of the distribution of a_i values, which was taken as a measurement of the equilibrium dynamics of the CA monolayer along the plane of the lattice (the breathing amplitude A_b).[24] The experimental data set was fitted to a Gaussian function to determine a_i and $a_b = A_b/2$:

$$y = y_0 + D\ \exp(-(2(a - a_i)/a_b)) \quad (1)$$

AFM-based analysis of the stiffness of CA monolayers

The mechanical properties of the CA^{wt} and CA mutant monolayers were determined essentially as previously described[30] with the same atomic force microscope and cantilevers used for imaging. The mechanical stiffness of each CA monolayer was quantified by determining its elastic constant, k_s. Shallow indentations (<2 nm) were performed to keep the protein lattice under the elastic regime. The k_s value was obtained from force–distance (Fz) traces by considering the cantilever as two ideal springs in series.[31] The actual elastic constant of the cantilever used in each experiment was determined using Sader's method.[32]

AFM-based analysis of the strength of CA monolayers subjected to point loads

The strength of the CA monolayer against disruption by a point load was quantified by determining the force F_r required for triggering a nonlinear event detected as a drop in the force in the Fz trace.[24,31] Indentations deep enough to reach the mica surface under the CA monolayer were performed. The F_r values for partial (F_{r1}) and complete (F_{r2}) disruption events were obtained.

AFM-based analysis of the resistance of CA monolayers to material fatigue

To induce material fatigue of the protein lattices, successive AFM images were taken under a force much lower than that required to trigger any disruption event that could be detected in the AFM images. The scanning size was 200 × 200 nm, the maximum applied force was set to 40 pN, and the indentation frequency was 0.7 min^{-1}. A number of experiments were performed in which both the E180A mutant and the CA^{wt} control were analyzed under the same conditions. Cyclic indentation of both monolayers was carried out until complete disassembly of the indented area of each monolayer. The remaining monolayer surface area as a function of time (or number of indentations) was determined using the Flooding tool included in the WSxM software.[28] The numerical data were fitted using the Hill function, as follows:

$$SA = SA_0 + (SA_F - SA_0)/(1 + (t_{50}/t)^n) \quad (2)$$

where SA_0 is the initial monolayer surface area (fixed at 100%), SA_F is the final monolayer surface area, t_{50} is the time required for disruption of half the indented monolayer, and n is a cooperative index.

The ratio between the time required, under the conditions of the experiment, for disruption of half the indented mutant monolayer and half the indented wt monolayer, $t_{50}^{mutant}/t_{50}^{wt}$, was taken as a measurement of the resistance to material fatigue of the mutant CA relative to non-mutated CA^{wt}.

Numerical data analysis

OriginPro 8 (Origin Lab Corporation) and Excel (Microsoft Corporation) were used for numerical data analysis. A two-tailed Student's t-test, with an α significance level equal to 0.05, was used to assess whether two given values of a mechanical parameter are different. No equal variance was assumed in this test.

Molecular graphics for structural analysis

Chimera[33] and WHATIF[34] software were used with PDB files 4XFX or 6SKN to represent structural models of CA and the CA protein lattice or to identify inter-subunit contacts in the lattice.

Results and discussion

Selection of CA amino acid residues for mutational analysis

The relationship between the atomic structure of protein-based assemblies and their mechanical properties can be studied by quantifying by AFM the variations in stiffness, strength, and fatigue resistance caused by very small structural alterations introduced by protein engineering.[16] In the present study, 7 CA amino acid residues involved in intermolecular interactions in the HIV-1 hexameric capsid protein lattice[35] were chosen for mutational analysis (Fig. 1 and Table 1). These residues sample the diversity of interfaces, intermolecular enthalpic interactions (van der Waals contacts, hydrogen bonds, ionic interactions), and the entropic hydrophobic effect that contribute to keep the CA subunits bound to each other with a certain chemical affinity. Those 7 residues were also chosen because they have a biological role in the HIV infectious cycle. They are highly conserved between HIV-1 variants, and they influence the stability of the HIV-1 protein capsid[36,37] and/or the CA-CA binding affinity.[27,38] This knowledge could help interpreting the results of the mechanical analysis performed in the present study.

Table 1 Engineered CA protein mutants

CA mutant	Intermolecular interactions established by the original residue[a]			Conservation in HIV-1 of the original residue[b] (%)
	H-bond	vdW (C–C)	Ionic	
P38A		3 (2)		100%
E45A	1	2	1 attractive	99%
Q63A	1	1		100%
V165A		2 (2)		99%
S178A	1	2		99% (*)
E180A	1	7	1 repulsive	97% (*)
Q192A		3 (1)		99%

[a] The interactions of different types in the atomic CA lattice structure (PDB 4XFX,[39]) that involve the side chain of the original residue (beyond Cβ), and that would be removed by mutation to alanine, were identified using the WHATIF software. The number of van der Waals (vdW) interactions between carbon atoms that contribute to protein–protein association through the hydrophobic effect are indicated in parenthesis. The E180A substitution actually increased the CTD-CTD dimerization affinity because the E180 of both monomers are involved in a mutual charge–charge repulsion.[27] Cutoff distances considered are 3.8 Å between electronegative atoms for hydrogen bonds (H-bonds); the sum of the vdW atomic radii plus 0.5 Å for vdW interactions; and 5 Å for ionic (charge–charge) interactions. [b] Percent conservation of each residue among the HIV-1 variants whose CA sequences were reported within the last 10 years. Values refer to absolute conservation, except those labelled with an asterisk, which correspond to chemical conservation (S or T for 178; E or D for 180).

The strategy followed was based on the individual and specific removal, through site-directed mutagenesis to alanine, of the targeted amino acid side chains (beyond the Cβ), without introducing any other chemical group. In this way, the intermolecular interactions established by each tested side chain would be removed without introducing other interactions, and with a minimal probability of substantially distorting the protein main chain conformation.

The CA protein mutants and the non-mutated CA^{wt} protein control were expressed, purified and used to build two-dimensional, one molecule-thick, flat protein assemblies that reproduce the hexameric CA lattice in the authentic HIV-1 capsid.[24,25] The CA monolayers were allowed to self-assemble in a physiological buffer (phosphate-buffered saline, PBS, pH = 7.4) at ambient temperature (25 °C) onto a suitable solid substrate (exfoliated mica).[24] The assembled monolayers were imaged by AFM to assess their supramolecular architecture and check their structural integrity. All 7 self-assembled mutant CA monolayers showed the exact same hexagonal

protein lattice as the CA^{wt} control (Fig. 1C). The monolayers virtually covered 100% of the substrate surface, and no lattice defects were discerned. The intact CA monolayers, always in PBS at room temperature, were then subjected to mechanical analysis as described below.

Effect of removing intermolecular interactions on the mechanical stiffness of a 2D protein nanostructure

For quantifying mechanical stiffness, relatively shallow indentations of the CA monolayers with the AFM tip were performed under the elastic regime. Every indentation of any CA monolayer was <2 nm deep (<30% of the protein material thickness), and was performed at a speed of 60 nm s^{-1}, using the same conditions for all CA mutants and the CA^{wt} control. The elastic constant k_s of each monolayer was determined from the slope of the linear region of the force–distance (*Fz*) traces as described in Experimental. Depending on the CA variant, between 60 and 100 *Fz* traces were analyzed. In each case, the k_s values obtained were averaged, and the ratio between the average k_s for the CA mutant and the average k_s for CA^{wt} control was obtained (Table 2 and Fig. 2).

Table 2 k_s values for CA^{wt} and engineered CA monolayers

CA protein	N^a	$k_s{}^b$ (N m^{-1})	$p_{k_s}{}^c$
CA^{wt}	100	0.37 ± 0.01	—
P38A	83	0.31 ± 0.01	3.97×10^{-7}
E45A	73	0.32 ± 0.01	1.13×10^{-9}
Q63A	81	0.30 ± 0.01	9.86×10^{-5}
V165A	60	0.32 ± 0.01	4.19×10^{-3}
S178A	79	0.33 ± 0.01	2.01×10^{-3}
E180A	78	0.36 ± 0.01	0.284
Q192A	63	0.30 ± 0.01	2.94×10^{-9}

[a] Number of *Fz* traces analyzed. [b] Average value ± standard error. Standard errors actually ranged between 0.005 and 0.009 and have been rounded to two decimal values. [c] *p*-Value obtained in a Student *t*-test for the difference in k_s between each mutant CA and CA^{wt} using $\alpha = 0.05$.

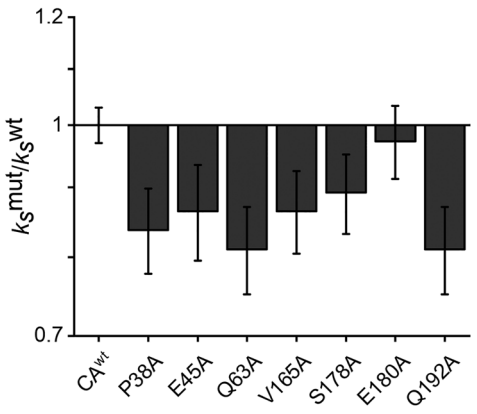

Fig. 2 k_s CA mutant/k_s CA^{wt} ratios for engineered CA monolayers. The reference k_s value determined for CA^{wt} was $k_s = 0.37 \pm 0.01$ N m^{-1}. The standard error values are indicated.

All 7 tested amino acid substitutions in CA led to a decrease in the stiffness of the protein material (as revealed by a lower k_s value). This decrease ranged from a nearly negligible effect (3%) for E180A, up to a substantial one (23%) for Q63A and Q192A. These results indicate that removal of different types of intermolecular interactions at any of the different intermolecular interfaces can decrease the stiffness of this nanostructured protein material.

Effect of removing different intermolecular interactions on the lateral conformational flexibility of a 2D protein nanostructure at equilibrium

The elastic constant k_s, determined by AFM for each CA monolayer as indicated above provided a measurement of its relative stiffness along the perpendicular to its surface. A force-based procedure for determining the stretchability along the plane of the protein monolayer could not be implemented. Instead, we estimated the conformational flexibility of the monolayer along its plane, by determining by AFM imaging the relative mobility at equilibrium of the CA hexamers that form the lattice.

The distances between many pairs of neighbor hexamers in each mutant CA lattice and the CA^{wt} control were determined from high-resolution AFM images of the corresponding protein monolayer.[24] Depending on the CA variant, between 249 and 528 distance measurements were obtained. From this data set, the equilibrium (average) distance between the centers of neighbor hexamers (the lattice parameter a_i) was determined for each mutant CA lattice, and compared to the a_i value obtained for the CA^{wt} lattice control in the same set of experiments (Fig. 3A). The a_i values for the different mutants ranged between 2% lower and 2% higher than the non-mutated control. Thus, none of the mutations had a significant effect on the equilibrium distance between CA hexamers in the protein lattice, whose architecture remained unaltered.

Then, the data set of distance values between hexamer pairs for each CA variant was fitted to a Gaussian distribution as described in Experimental. The width of the distance distribution, or breathing amplitude A_b, was determined.[24] The ratio between the A_b value for the CA mutant and the A_b value for CA^{wt} was then obtained as a parameter related to the effect of each tested mutation on the lateral flexibility of the CA lattice at equilibrium[24] (Fig. 3B).

As observed for the decreased stiffness determined by indentation of the protein lattice, all 7 tested mutations led to an increase in the breathing amplitude of the lattice, albeit to different extents. The range of increased breathing amplitude A_b for the ensemble of mutants (4%–21%) was similar to the range of decreased stiffness (3%–23%). The precision of these measurements is not enough to assess whether there is a quantitative correlation between a decrease in k_s and an increase in A_b. However, the results do indicate that removal of different types of intermolecular interactions decreases the stiffness along the vertical dimension to fairly comparable extents than it increases the equilibrium conformational flexibility along the horizontal dimension of this protein material.

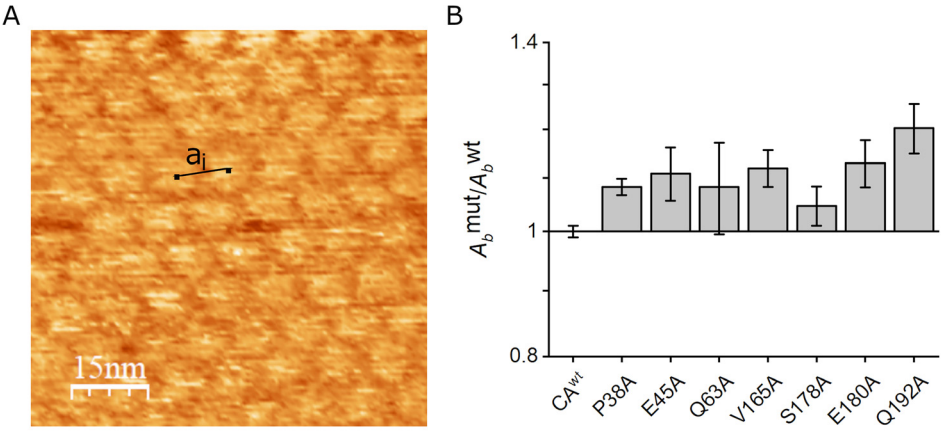

Fig. 3 Lateral flexibility of CA mutant monolayers compared to CA^{wt}. (A) Definition of the a_i parameter of a CA protein lattice. The scale bar corresponds to 15 nm. (B) A_b mutant/A_b^{wt} ratio for each tested protein lattice. The reference A_b value determined for CA^{wt} was A_b = 1.93 ± 0.01 nm. The standard error values are indicated.

Effect of removing different intermolecular interactions on the strength of a 2D protein nanostructure

For quantifying the relative strength of each CA monolayer when subjected to a point load, indentations deep enough to reach the substrate surface underneath were performed with the AFM tip. The strength of the CA monolayer against disruption was quantified by determining the force F_r required for triggering a nonlinear event, detected in the *Fz* trace as a drop in the applied force.[24] A previous study had shown that deep indentations of the CA^{wt} monolayer led, in most cases, to two successive disruption events. During the first event, that occurred at a lower force (F_{r1}), some interactions between subunits in the same CA hexamer may be disrupted; during the second event, that occurred at a higher force (F_{r2}), some interactions between CA hexamers may be additionally disrupted, leading to complete breakage of the monolayer at the indented point.[24]

Depending on the CA variant, between 44 and 86 *Fz* traces were analyzed. In each case, the F_{r1} and F_{r2} values obtained were separately averaged, and the ratio between the average F_{r1} or F_{r2} value for the CA mutant and the corresponding average F_{r1} or F_{r2} value for the CA^{wt} control was obtained (Table 3 and Fig. 4).

The effects of each tested amino acid substitution on the F_{r1} value were very similar to the effects on the F_{r2} value. Most (5 out of 7) tested mutations led to a decrease in the strength of the protein material, albeit to significantly different extents. Depending on the CA mutant, the F_{r2} value was between 8% and 25% lower than the wt control. In contrast, the two remaining substitutions led to significant increases in the mechanical strength of the CA monolayer, 10% for Q192A, and as much as 63% for E180A. This constitutes a particularly revealing result, as the E180A and Q192A mutations were previously shown to increase, instead of decrease, the association affinity between CA subunits. Moreover, an experimental thermodynamic double mutant cycle had shown that the E180 residue is involved in charge–charge repulsions between CA subunits, which would be eliminated by the E180A mutation.[27] The Q192A mutation may also alleviate some CA-CA repulsions.[27] These results indicate that removal of different types of attractive intermolecular interactions in any of the different interprotein interfaces can decrease the mechanical strength; and that, conversely, the removal of repulsive charge–charge intermolecular interactions can actually increase the mechanical strength of this nanostructured protein material.

Table 3 F_{r1} and F_{r2} values for CA^{wt} and engineered CA monolayers

CA protein	N^a	F_{r1} [b] (nN)	$p_{F_{r1}}$ [c]	F_{r2} [b] (nN)	$p_{F_{r2}}$ [c]
CA^{wt}	86	0.33 ± 0.01	—	0.63 ± 0.01	—
P38A	44	0.30 ± 0.01	2.51×10^{-2}	0.58 ± 0.01	8.20×10^{-3}
E45A	37	0.28 ± 0.01	7.96×10^{-6}	0.58 ± 0.01	2.69×10^{-3}
Q63A	53	0.22 ± 0.01	1.18×10^{-17}	0.47 ± 0.01	1.45×10^{-15}
V165A	47	0.30 ± 0.01	9.77×10^{-3}	0.57 ± 0.01	7.11×10^{-5}
S178A	64	0.28 ± 0.01	7.83×10^{-6}	0.53 ± 0.01	1.13×10^{-10}
E180A	84	0.53 ± 0.02	6.79×10^{-16}	1.03 ± 0.03	1.01×10^{-21}
Q192A	81	0.36 ± 0.01	4.13×10^{-2}	0.69 ± 0.01	5.46×10^{-5}

[a] Number of *Fz* traces analyzed. [b] Average value ± standard error. [c] *p*-Value obtained in a Student *t*-test for the difference in F_r between each mutant CA and CA^{wt} using $\alpha = 0.05$.

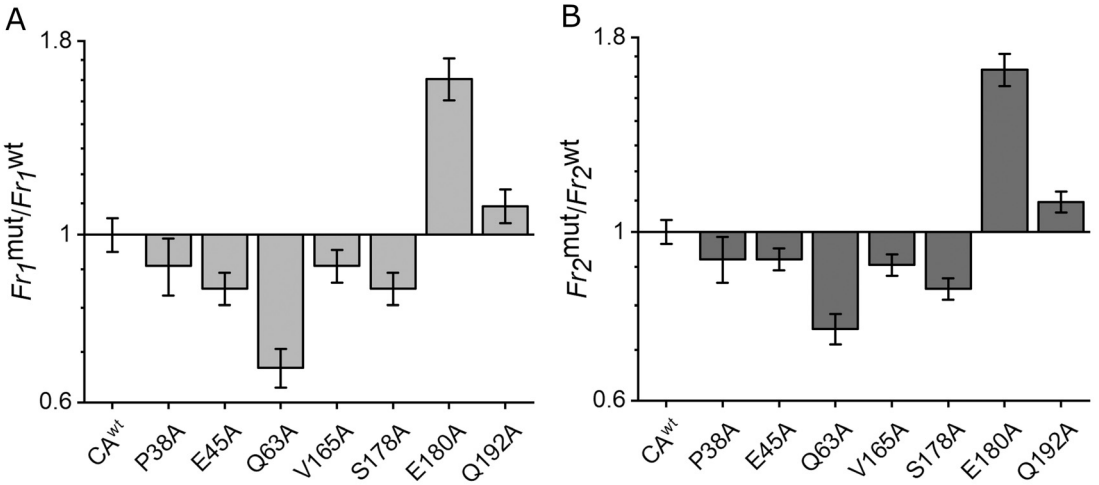

Fig. 4 F_r CA mutant/F_r CA^{wt} ratios for engineered CA monolayers. (A), F_{r1} ratios. (B) F_{r2} ratios the reference values obtained for CA^{wt} was F_{r1} = 0.33 ± 0.01 nN and F_{r2} = 0.63 ± 0.01 nN. The standard error values are indicated.

Effect of removing a repulsive ionic interaction on the resistance to fatigue of a 2D protein nanostructure subjected to a moderate cyclic load

As the E180A mutation led to a large increase in the strength of the CA monolayer subjected to a point load, we wondered whether the same mutation could also substantially increase the resistance to fatigue of this nanostructured 2D material when a much lower load was cyclically applied.

The resistance of the engineered E180A CA protein monolayer to material fatigue was compared to that of the CA^{wt} monolayer control by scanning 200 × 200 nm areas of the monolayers, with a maximum applied force set to 40 pN, and an indentation frequency of 0.7 min^{-1}. The percent monolayer surface area subjected to fatigue that remained assembled as a function of time (or number of indentations) (Fig. 5) was determined using the Flooding tool included in the WSxM software.[28] The ratio between the time required, under the conditions of the experiment, for disruption of half the indented mutant monolayer and that needed for disruption of half the indented wt monolayer, t_{50}^{mut}/t_{50}^{wt}, was determined. This parameter was used for a quantitative measurement of the resistance to material fatigue of the mutant CA lattice relative to non-mutated CA^{wt} lattice.[30]

Seven independent experiments were performed with E180A monolayers and CA^{wt} monolayer controls. Fig. 5A shows images of the two monolayers taken at different times during a representative experiment. The CA lattice surface area remaining as a function of time in three representative experiments is shown in Fig. 5B. When compared to the CA^{wt} monolayer, the E180A mutant monolayer showed, in each independent experiment, a substantially increased resistance against disruption by material fatigue (by 44–76%). The moderate variation in the absolute t_{50} values between experiments were likely due, in part, to a difference in the number of undetectable, minor initial defects in the individual monolayers analyzed. The t_{50}^{mut}/t_{50}^{wt} ratio (average plus standard deviation), obtained as described in Experimental, are indicated in Fig. 5C. On average, the engineered E180 monolayer was 55% (±15%) more resistant to fatigue than the wt monolayer.

A second series of 4 experiments was performed under similar conditions to those used for the first series of experiments described above. This first and second series of experiments yielded very similar results (averaged increase in resistance to fatigue 55% and 40%, respectively). The ensemble of results show that mutation E180A in CA, which removes a repulsive charge–charge interaction between subunits in the CA monolayer, increases to a remarkable extent (by ~50%) the resistance to fatigue of this nanostructured protein material.

Molecular determinants of stiffness, strength and resistance to fatigue of a 2D nanostructured protein material

The AFM-based mutational analysis performed in this study provides insights into the role of different amino acid residues, and the intermolecular interactions they establish, in determining the mechanical properties of a 2D protein nanostructure. The protein sheet is only very weakly held by the substrate, and the mutations tested affect residues at the interfaces between CA subunits in the 2D lattice, far from the substrate surface. The correlation between removal of either attractive or repulsive interactions (observed in the absence of substrate) and, respectively, decreased or increased strength (tested in the presence of substrate) suggests that the effect of the mutations may be intrinsic to the protein material. However, the experiments cannot rule out the possibility that the type of substrate could influence somewhat the effect the mutations had on the observed mechanical properties. For most envisaged applications, such as tissue regeneration, the protein 2D nanostructure will certainly require a stable inert matrix material. The analysis described here sampled 7 residues that participate in different types of non-covalent interactions involved in joining the individual protein molecules in

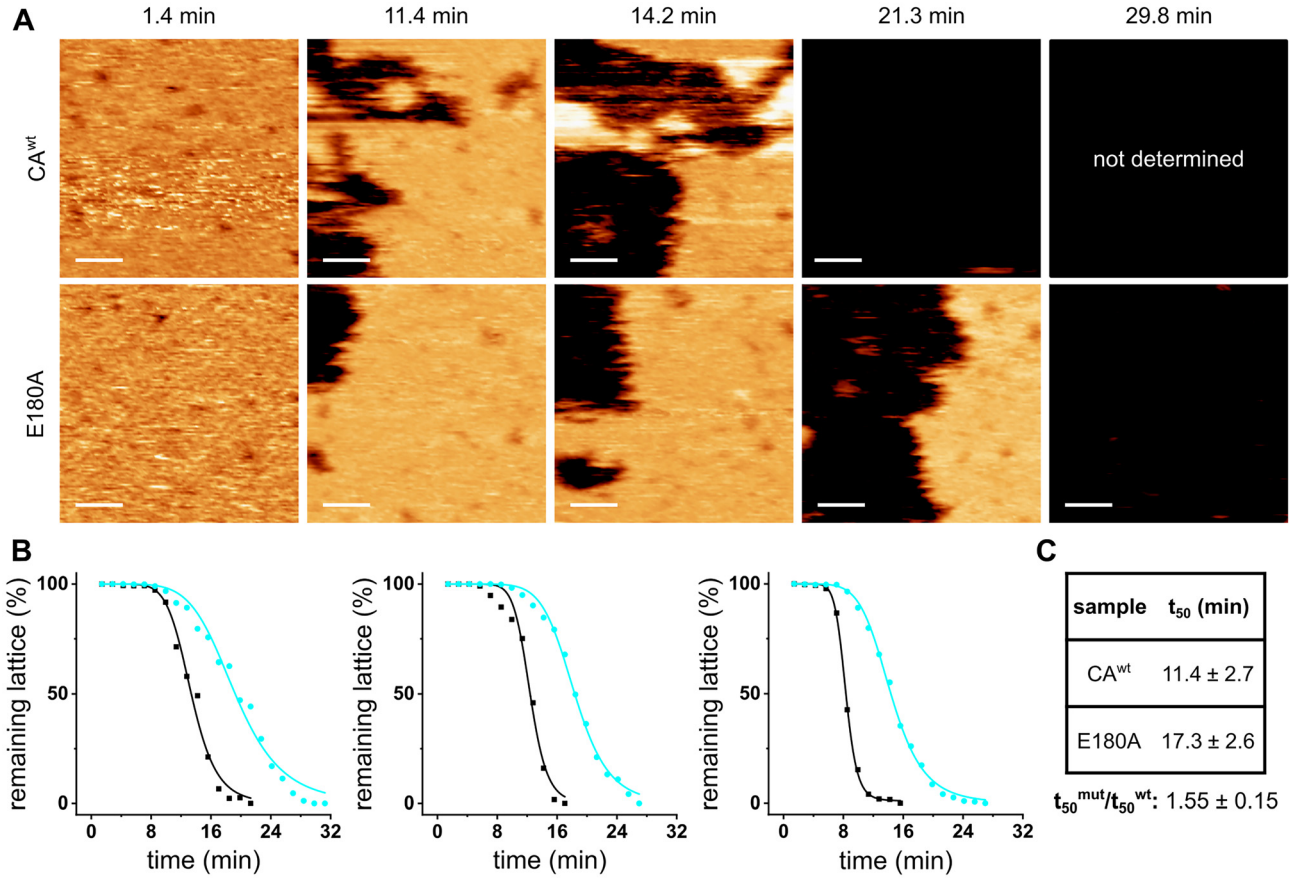

Fig. 5 Effect of the E180A amino acid substitution on the resistance of the CA monolayer to material fatigue. (A) AFM images obtained in a representative experiment at different times under material fatigue conditions. The scale bars represent 40 nm. (B) Percent surface area of the E180A mutant CA monolayer (cyan circles) and of the CA^{wt} monolayer control (black squares) that remained non-dissociated as a function of time under cyclic indentations leading to material fatigue. Each plot corresponds to a different experiment. The data (points) were fitted as indicated in Experimental. (C) t_{50} values (average ± standard deviation) for CA^{wt} and mutant E180A, and t_{50}^{mut}/t_{50}^{wt} ratio (average ± standard deviation), obtained from the data represented in panel B.

the array through any one of 3 different interfaces (NTD-NTD, NTD-CTD and CTD-CTD). The insights provided are discussed next.

Stiffness and intrinsic deformability. Every tested mutation led to a decrease in the k_s of the material when subjected to a point load under the elastic regime. As the architecture and dimensional parameters of the protein array were not changed by any of the mutations, a decrease in the k_s value (stiffness) implies the same decrease in the Young's modulus of elasticity E. Thus, every tested mutation decreases the stiffness of the 2D nanostructure and increases the reversible intrinsic deformability of the protein material. This result can be rationalized because every mutation tested removed some non-covalent interactions between each pair of protein subunits in the array. This would provide more degrees of freedom for the reversible displacement of each subunit relative to their neighbor subunits, facilitating the elastic deformation of the monolayer in response to shallow indentations.

However, some other results were less predictable. H-bonds are directional, whereas vdW interactions, including "hydrophobic" carbon–carbon contacts, are not. Thus, a higher stiffness decrease could be predicted if H-bonds are removed instead of vdW contacts. In fact, amino acid substitutions E45A, Q63A, and S178A removed one hydrogen bond each (plus 1–2 vdW contacts) between pairs of protein subunits, but they decreased the stiffness of the array to a similar extent than P38A, Q165A, and Q192A, which removed 2–3 vdW contacts only. Another remarkable result is that substantial (up to 23%) stiffness decreases were achieved by removing few, relatively weak non-covalent interactions between each protein pair in the array (one H-bond and/or 1–2 C–C hydrophobic contacts, together with 1–2 additional vdW interactions). Also, the decrease in stiffness of the CA monolayer by any tested mutation, as determined by indentation along the perpendicular to the protein lattice plane, was accompanied by an increase in the conformational flexibility of the monolayer along the lattice plane.

The above results are in line with those we obtained when studying the effect of amino acid substitutions on the stiffness and conformational dynamics of small, spherical

nanoparticles from HIV-1-unrelated viruses.[40,41] The available evidence indicates that removal of even a few interactions in a viral protein-made nanostructure, irrespective of the type(s) of interaction removed, may elicit quite subtle conformational rearrangements. Such rearrangements may increase the conformational dynamics of the particle at equilibrium, leading to a corresponding decrease in stiffness as determined under a point load.[16]

It must be emphasized that those results were obtained with natural protein nanostructures that form the capsids of different viruses and have been, thus, subjected to selective pressures and biological evolution. There is experimental evidence that the inter-related changes in stiffness, conformational flexibility and propensity for conformational rearrangements of viral capsids have been optimized through structural changes elicited by mutation to provide a selective advantage for virus survival.[9,16] It remains to be investigated whether the individual removal of intersubunit interactions in artificial protein arrays, whose structure and physical properties have not been subjected to biological evolution, would lead to changes in stiffness similar to the ones determined in this study.

Strength. Removal of attractive intermolecular interactions through mutation led to a decrease in the force required for local disruption of the CA lattice when subjected to a deep enough indentation. Those mutations removed some enthalpic interactions and/or reduced the hydrophobic effect that kept together each pair of protein subunits in the array. Thus, less interactions remained to be disrupted when a point load was applied. In contrast, removal of repulsive electrostatic interactions led to an increase in the force required for lattice disruption. Thus, the mechanical strength of this protein 2D nanostructure could be modulated by removing attractive interactions (lowering strength) and by removing repulsive interactions (increasing strength).

No correlation, however, was observed between the decrease in stiffness and the decrease in mechanical strength of the monolayer as a consequence of the different amino acid substitutions tested and intermolecular interactions removed. Whereas all mutant CAs formed arrays of decreased stiffness relative to the CA^{wt} control, a much higher variability was observed regarding their relative mechanical strength. In particular, CA mutants E180A and Q192A self-assembled into protein arrays with the same architecture, but showed a higher mechanical strength than the CA^{wt} control. We had already observed this lack of correlation between changes in stiffness and strength for unrelated, small spherical virus nanoparticles.[42] These two mechanical properties of protein nanostructures rely on different physico-chemical foundations.[16] Thus, although for most tested mutations a decrease in stiffness of this nanostructured array was accompanied by a decrease in its strength, these two properties are not intrinsically linked in this or other protein-based materials.

An experimental, rigorous thermodynamic double mutant cycle revealed a mutual coulombic repulsion between the negatively charged carboxylates of the E180 residues at the CTD-CTD interface between CA monomers.[27] The E180A mutation eliminates the E180 carboxylates and their mutual repulsion, increasing the free energy of CA-CA association through the CTD-CTD interface.[38] As a consequence, a higher mechanical force could be expected to be required for disruption of the CA array, as experimentally observed in the present study. The Q192A mutation also increased the free energy of association between CA monomers through the CTD-CTD interfaces. This mutation could create a cavity at the CTD-CTD interface, leading to a local conformational rearrangement that would increase the distance between the positively charged residues R154 of one monomer and K199 of the other monomer, thus reducing their mutual repulsion.[38] Consistent with these observations, the Q192A mutation, like the E180A mutation, also increased the strength of the CA array, albeit to a lower extent. To sum up, the increased mechanical strength of the E180A and Q192A mutant arrays was associated to an increased chemical affinity between CA subunits and could be traced, at least in the E180A case, to the removal of repulsive interactions between subunits in the CA protein lattice.

Resistance to material fatigue. The structural basis for the susceptibility of nanostructured protein materials to material fatigue is virtually unknown. A working hypothesis[16] proposes that cyclic application to a protein nanoarray of a force well below the breaking force F_r may transiently disrupt a small number of the weak non-covalent interactions between protein subunits. The high chemical and sterical complementarity between the subunits will lead, when the load is removed, and given enough time before the next load cycle, to the regaining of the lost interactions, resulting in a fully reversible, elastic deformation of the array. However, if the load is cyclically applied at a high enough frequency, there may be not enough time for every broken interaction in the previous cycle to be re-established. Subsequent load cycles will lead to an increasing number of broken intersubunit interactions being unable to recover, resulting in an enlargement and merging of intermolecular openings ("cracks") in the material, until complete protein–protein interfaces are disrupted. Eventually, whole protein subunits would be removed until the perturbed region of the protein nanoarray becomes fully disintegrated.[16]

The mutual coulombic repulsion between E180 residues of neighbor subunits in the CA protein lattice would favor the enlargement of the intermolecular "cracks" being created under cyclic load, leading to a relatively high susceptibility to material fatigue. The absence of those repulsive interactions in the E180A mutant lattice would facilitate the recovery of some of the intersubunit interactions being disrupted under cyclic load, leading to the observed, substantially increased resistance of this engineered protein nanostructured material to fatigue.

The results of this study are relevant also from an applied perspective. We have recently shown that the mechanical strength and resistance to fatigue of the CA-based nanostructured coating can be increased by specific binding of some small organic molecules, including antiviral or proviral agents.[30] However, from a practical standpoint it may be clearly unfeasible to rely on the non-covalent binding of a small molecule to increase the mechanical resistance of a bio-

material. Irreversible modification of the material through chemical reactions (*e.g.*, by covalent crosslinking) may also present serious issues, such as batch-to-batch reproducibility, increased production costs, and complex quality control. In another recent study, we showed that genetic introduction through cysteine substitutions of a "chain mail" based on covalent disulfide bonds between protein subunits led to a CA-based nanostructured coating that showed increased mechanical strength and outstanding resistance to material fatigue.[43] Still, while not an expected serious issue, preservation of the chain mail requires the control of redox conditions for maintaining an oxidizing environment. In contrast, introduction of a genetically-encoded structural modification in mutant E180A results in an intrinsically strong protein material that could be reproducibly obtained, eliminating batch-to-batch variability and simplifying production and quality control. The E180A CA protein, like the non-mutated CA, can be readily obtained in large quantities and has no tendency to form unspecific aggregates even at very high concentrations, far superior than those needed for its assembly. In addition, the 2D nanosheet can fully cover large substrate areas provided enough protein is used. This study provides proof-of-concept for an alternative genetic strategy to the introduction of disulfide bonds to increase the intrinsic mechanical strength and resistance to fatigue of the same nanostructured protein material. This strategy was based on the optimization of the ionic interactions between subunits, especially through the removal of any coulombic repulsions present in the starting material.

Conclusion

Removal of chemical groups involved in different types of attractive non-covalent interactions between molecular components of a 2D natural protein nanoarray invariably decreased its stiffness, at the expense of also reducing its strength against disruption by point loads. However, removal by protein engineering of repulsive charge–charge intermolecular interactions in the original material led to large increases in its strength and resistance to fatigue, without compromising its reversible deformability. The results with this model protein nanoarray derived from a virus capsid encourage the optimization, through genetic means, of the ionic interactions between protein components of protein nanomaterials as a general strategy to increase their mechanical robustness. We also envisage the combined introduction by protein engineering of intersubunit disulfide bonds and optimization of ionic interactions to further increase the intrinsic mechanical strength and fatigue resistance of protein nanoarrays for medical or technological applications.

Author contributions

J. E. performed nearly all experiments. J. C. G.-R. performed some experiments. J. E., J. C. G.-R., A. V. and M. G. M. analyzed and discussed results. M. G. M. and A. V. designed and supervised the study, and M. G. M. wrote the paper with major input from A. V. and contributions from the other authors.

Conflicts of interest

There is no conflict of interests to declare.

Data availability

The data of the manuscript are available upon request from the authors.

Acknowledgements

This work was funded by a Ministerio de Ciencia e Innovación/FEDER EU grant to M. G. M. (PID2021-126973OB-I00). Institutional grants from the Severo Ochoa Program for Centers of Excellence in R&D (CEX2021-00154-S) and from the Fundación Ramón Areces are also acknowledged. J. E. was the recipient of a FPI research contract from MICINN. M. G. M. is an associate member of the Institute for Biocomputation and Physics of Complex Systems, Zaragoza, Spain.

References

1 *Protein-based Engineered Nanostructures*, book series *Advances in Experimental Medicine and Biology*, ed. A. L. Cortajarena and T. Z. Grove, Springer, Switzerland, 2016, vol. 940.
2 I. W. Hamley, Protein assemblies: nature-inspired and designed nanostructures, *Biomacromolecules*, 2019, **20**, 1829–1848.
3 *Protein Nanotechnology*, book series Methods in Molecular Biology, ed. J. A. Gerrard, L. Domigan, Humana Press, NY, 3rd edn, 2020, vol. 2073.
4 S. Ding, N. Zhang, Z. Lyu, W. Zhu, Y. C. Chang, X. Hu, D. Du and Y. Lin, Protein-based nanomaterials and nanosystems for biomedical applications: a review, *Mater. Today*, 2021, **43**, 166–184.
5 J.-T. Zhang, J. Ma, R. K. Kankala, Q. Yu, S.-B. Wang and A.-Z. Chen, Recent advances in fabrication of well-organized protein-based nanostructures, *ACS Appl. Bio Mater.*, 2021, **4**, 4039–4048.
6 M. G. Mateu and A. Valbuena, Engineering and bio/nanotechnological applications of virus particles. in *Structure and Physics of Viruses*, ed. M. G. Mateu, book series *Subcellular Biochemistry*, Springer Nature, Switzerland, 2nd edn, 2024, vol. 105, pp. 823–878.
7 M. G. Mateu, Assembly, engineering, and applications of virus-based protein nanoparticles. in *Protein-based engineered nanostructures*, ed. A. L. Cortajarena and T. Z. Grove,

book series *Advances in Experimental Medicine and Biology*, Springer, Switzerland, 2016, Vol. 940, pp. 83–120.

8 R. A. L. Jones, Challenges in soft nanotechnology, *Faraday Discuss.*, 2009, **143**, 9–14.

9 P. J. de Pablo and M. G. Mateu, Mechanical properties of viruses. in *Structure and Physics of Viruses*, ed. M. G. Mateu, book series *Subcellular Biochemistry*, Springer, Switzerland, 2nd edn, 2024, vol. 105, pp. 823–878.

10 Y. Kurotani and H. Tanaka, Fatigue fracture mechanism of amorphous materials from a density-based coarse-grained model, *Commun. Mater.*, 2022, **3**, 67.

11 A. Ortega-Esteban, A. J. Pérez-Berná, R. Menéndez-Conejero, S. J. Flint, C. San Martín and P. J. de Pablo, Monitoring dynamics of adenovirus disassembly induced by mechanical fatigue, *Sci. Rep.*, 2013, **3**, 1434.

12 N. Martín-González, A. Gómez-González, M. Hernando-Pérez, M. Bauer, U. F. Greber, C. San Martín and P. J. de Pablo, Adenovirus core protein V reinforces the capsid and enhances genome release from disrupted particles, *Sci. Adv.*, 2023, **9**, eade9910.

13 A. Valbuena and M. G. Mateu, Kinetics of a surface-driven self-assembly and fatigue-induced disassembly of a virus-based nanocoating, *Biophys. J.*, 2017, **112**, 663–673.

14 F. J. O'Brien, Biomaterials and scaffolds for protein engineering, *Mater. Today*, 2011, **14**, 88–95.

15 R. Putri, J. J. Cornelissen and M. S. Koay, Self-assembled cage-like protein structures, *ChemPhysChem*, 2015, **16**, 911–918.

16 M. G. Mateu, Virus mechanics: a structure-based biological perspective, in *Physical Virology*, ed. M. Comas-García and S. Rosales-Mendoza, book series *Springer Series in Biophysics*, Springer, Switzerland, 2023, vol. 24, pp. 237–282.

17 X. Liu, L. Zhang, X. Cui, Q. Zhang, W. Hu, J. Du, H. Zeng and Q. Xu, 2D material nanofiltration membranes: from fundamental understandings to rational design, *Adv. Sci.*, 2021, **8**, e2102493.

18 Y. Zheng, X. Hong, J. Wang, L. Feng, T. Fan, R. Guo and H. Zhang, 2D Nanomaterials for tissue engineering and regenerative nanomedicines: recent advances and future challenges, *Adv. Healthcare Mater.*, 2021, **10**, e2001743.

19 Z. Cao, Y. Bian, T. Hu, Y. Yang, Z. Cui, T. Wang, S. Yang, X. Weng, R. Liang and C. Tan, Recent advances in two-dimensional nanomaterials for bone tissue engineering, *J. Materiomics*, 2023, **9**, 930–958.

20 C. Zheng, N. Alvisi, R. Jan de Haas, Z. Zhang, H. Zuilhof and R. de Vries, Modular design for proteins assembling into antifouling coatings: case of gold surfaces, *Langmuir*, 2023, **39**, 9290–9299.

21 C. Jiang, G. Wang, R. Hein, N. Liu, X. Luo and J. J. Davis, Antifouling strategies for selective in vitro and in vivo sensing, *Chem. Rev.*, 2020, **120**, 3852–3889.

22 J. Raff, S. Matys, M. Suhr, M. Vogel, T. Günther and K. Pollmannen, S-layer-based nanocomposites for industrial applications, in *Protein-Based Engineered Nanostructures*, ed. A. L. Cortajarena and T. Z. Grove, *Advances in Experimental Medicine and Biology*, Springer, Switzerland, 2016, vol. 940, pp. 245–279.

23 J. F. Matthaei, F. DiMaio, J. J. Richards, L. D. Pozzo, D. Baker and F. Baneyx, Designing two-dimensional protein arrays through fusion of multimers and interface mutations, *Nano Lett.*, 2015, **15**, 5235–5239.

24 A. Valbuena and M. G. Mateu, Quantification and modification of the equilibrium dynamics and mechanics of a viral capsid lattice self-assembled as a protein nanocoating, *Nanoscale*, 2015, **7**, 14953–14964.

25 J. R. Perilla, J. A. Hadden-Perilla, A. M. Gronenborn and T. Polenova, Integrative structural biology of HIV-1 capsid protein assemblies: combining experiment and computation, *Curr. Opin. Virol.*, 2021, **48**, 57–64.

26 H.-B. Pang, L. Hevroni, N. Kol, D. M. Eckert, M. Tsvitov, M. S. Kay and I. Rousso, Virion stiffness regulates mature HIV-1 entry, *Retrovirology*, 2013, **10**, 4.

27 M. del Alamo and M. G. Mateu, Electrostatic repulsion, compensatory mutations, and long-range non-additive effects at the dimerization interface of the HIV capsid protein, *J. Mol. Biol.*, 2005, **345**, 893–906.

28 I. Horcas, R. Fernández, J. M. Gómez-Rodríguez, J. Colchero, J. Gómez-Herrero and A. M. Baro, WSXM: A software for scanning probe microscopy and a tool for nanotechnology, *Rev. Sci. Instrum.*, 2007, **78**, 013705.

29 F. Moreno-Herrero, J. Colchero, J. Gómez-Herrero and A. M. Baró, Atomic force microscopy contact, tapping, and jumping modes for imaging biological samples in liquid, *Phys. Rev. E Stat. Nonlin. Soft Matter Phys.*, 2004, **69**, 031915.

30 S. Domínguez-Zotes, A. Valbuena and M. G. Mateu, Antiviral compounds modulate elasticity, strength and material fatigue of a virus capsid framework, *Biophys. J.*, 2022, **121**, 919–931.

31 I. L. Ivanovska, P. J. de Pablo, B. Ibarra, G. Sgalari, F. C. MacKintosh, J. L. Carrascosa, C. F. Schmidt and G. J. L. Wuite, Bacteriophage capsids: Tough nanoshells with complex elastic properties, *Proc. Natl. Acad. Sci. U. S. A.*, 2004, **101**, 7600–7605.

32 J. E. Sader, J. W. M. Chon and P. Mulvaney, Calibration of rectangular atomic force microscope cantilevers, *Rev. Sci. Instrum.*, 1999, **70**, 3967–3969.

33 E. F. Pettersen, T. D. Goddard, C. C. Huang, G. S. Couch, D. M. Greenblatt, E. C. Meng and T. E. Ferrin, UCSF Chimera-a visualization system for exploratory research and analysis, *J. Comput. Chem.*, 2004, **13**, 1605–1612.

34 G. Vriend, WHATIF. a molecular modeling and drug design program, *J. Mol. Graphics*, 1990, **8**, 52–56.

35 J. Escrig, I. Marcos-Alcalde, S. Domínguez-Zotes, D. Abia, P. Gómez-Puertas, A. Valbuena and M. G. Mateu, Structural basis for alternative self-assembly pathways leading to different human immunodeficiency virus capsid-like nanoparticles, *ACS Nano*, 2024, **18**, 27465–27478.

36 R. Yang, I.-J. Shi, L. Byeon, J. Ahn, J. H. Sheehan, J. Meiler, A. M. Gronenborn and C. Aiken, Second-site suppressors of HIV-1 capsid mutations: restoration of intracellular activi-

ties without correction of intrinsic capsid stability defects, *Retrovirology*, 2012, **9**, 30.

37 E. L. Yufenyuy and C. Aiken, The NTD-CTD intersubunit interface plays a critical role in assembly and stabilization of the HIV-1 capsid, *Retrovirology*, 2013, **10**, 29.

38 M. del Alamo, J. L. Neira and M. G. Mateu, Thermodynamic dissection of a low affinity protein-protein interface involved in human immunodeficiency virus assembly, *J. Biol. Chem.*, 2003, **278**, 27923–27929.

39 A. T. Gres, K. A. Kirby, V. N. KewalRamani, J. J. Tanner, O. Pornillos and S. G. Sarafianos, X-ray crystal structures of native HIV-1 capsid protein reveal conformational variability, *Science*, 2015, **349**, 93–103.

40 P. J. P. Carrillo, M. Medrano, A. Valbuena, A. Rodríguez-Huete, M. Castellanos, R. Pérez and M. G. Mateu, Amino acid side chains buried along intersubunit interfaces in a viral capsid preserve low mechanical stiffness associated with virus infectivity, *ACS Nano*, 2017, **11**, 2194–2208.

41 A. Valbuena, A. Rodríguez-Huete and M. G. Mateu, Mechanical stiffening of human rhinovirus by cavity-filling antiviral drugs, *Nanoscale*, 2018, **10**, 1440–1452.

42 M. Medrano, A. Valbuena, A. Rodríguez-Huete and M. G. Mateu, Structural determinants of mechanical resistance against breakage of a virus-based protein nanoparticle at a resolution of single amino acids, *Nanoscale*, 2019, **11**, 9369–9383.

43 S. Domínguez-Zotes, M. A. Fuertes, A. Rodríguez-Huete, A. Valbuena and M. G. Mateu, A genetically engineered, chain mail-like nanostructured protein material with increased fatigue resistance and enhanced self-healing, *Small*, 2022, 2105456.